On problems of isoconversion data processing for reactions in Al-rich Al–MoO$_3$ thermites

Swati M. Umbrajkar, Chi-Mon Chen, Mirko Schoenitz *, Edward L. Dreizin

New Jersey Institute of Technology, Newark, NJ 07102, United States

ARTICLE INFO

ABSTRACT

Isoconversion processing of thermoanalytical data, while becoming more and more widely used, remains problematic when used indiscriminately. The exothermic reaction in a 4Al·MoO$_3$ nanocomposite thermite, prepared by arrested reactive milling, was investigated at heating rates ranging from 1 to 40 K/min. The data processing according to a number of traditional isoconversion methods (Kissinger, Friedman, Ozawa–Flynn–Wall), reveals distinct and experimentally reproducible nonlinear regions in the plots of their respective logarithmic function *vs.* inverse temperature, possibly indicating changes in reaction mechanism over this range of heating rates. More contemporary implementations of isoconversion algorithms give results that are substantially similar. In order to predict kinetic behavior under any heating conditions, especially outside the range of heating rates covered by experiments, a detailed mechanistic model of all involved processes is needed.

Published by Elsevier B.V.

1. Introduction

Isoconversion processing provides a convenient and practical means to extract quantitative kinetic information from thermoanalytical data/measurements. It has been originally conceived in the 1950s [1], with development continuing since then and through today, e.g. [2–5]. New and more sophisticated algorithms continue to be developed and published [6–9], and several commercial software packages make various variants of the method widely available, e.g. [10–14]. Inherent in the method is the assumption that the thermal activation of the process can either be described by a single activation energy or can be approximated by an effective activation energy. If the process is more complex, the effective activation energy determined will be a compound parameter that may change with reaction progress and temperature, representing the balance of concurrent processes contributing to the net reaction at a given time and temperature.

The use of this compound quantity has recently come under criticism as an ill-defined, and relatively meaningless parameter [15]. Proponents of the method counter with several arguments [16,17]. First, some isoconversion methods can be inverted, and therefore "model-free" kinetic data can be used to reconstruct

reaction rates and associated heat effects under arbitrary heating conditions. For engineering applications, this is frequently sufficient to model and design a specific process. Second, specifically in condensed-phase reactions it is often unclear what constitutes an elementary reaction step that would be associated with a unique set of Arrhenius parameters. Not least because of this, it is generally not feasible to design an experiment that separates the individual component reactions of a chemical process/net reaction. It is therefore usually suggested to use the data obtained from isoconversion processing as a starting point for the development of a more detailed and fundamental mechanistic model of the reaction in question [16]. Due to the difficulties isolating individual reaction steps, isoconversion-derived parameters will frequently be the best information available.

While theoretical limitations of the isoconversion processing are well documented, the authors feel that not enough studies have been published that show specific cases for which isoconversion processing does not lead directly to a useful reaction model. Detailed descriptions of such cases will enable researchers to better gauge how adequate or inadequate any specific set of measurements is for isoconversion processing, and how meaningful the obtained activation energies are.

The case presented here is the complex redox reaction in an off-stoichiometric Al–MoO$_3$ nanocomposite powder. With the recent development of novel reactive nanomaterials, including those employing thermite reactions [18–22], it became of significant interest to apply the kinetics information derived from thermal analysis to heating conditions at much higher rates. The objective

* Corresponding author at: Department of Chemical Engineering, New Jersey Institute of Technology University Heights, Newark, NJ 07102, United States. Tel.: +1 973 596 5260; fax: +1 973 596 8436.

E-mail address: schoenit@njit.edu (M. Schoenitz).

is to quantify ignition kinetics for such materials under conditions generally not accessible by thermal analysis methods. Likewise, quantification of aging behavior requires reliable extrapolation from thermal analysis experiments as well.

The reaction is studied here for fully dense nanocomposite powders with a composition of 4Al + MoO$_3$ (excess Al over the stoichiometric composition) prepared by arrested reactive milling (ARM). Detailed description of synthesis of reactive nanocomposite powders by ARM is available elsewhere [22–24]. The material used in this study and other similar nanocomposite materials are currently being developed for advanced reactive formulations to be used in propellants, explosives, and pyrotechnics. Previous work has shown that the general sequence of reactions in such material includes decomposition of MoO$_3$ into MoO$_2$ and O and diffusion of oxygen ions to Al through layers of different polymorphs of Al$_2$O$_3$ and possibly through MoO$_2$ [23]. At higher temperatures, formation of ternary oxides, Al$_2$MoO$_6$ was observed. A multistage reaction like this is likely to be governed by multiple interacting thermally activated processes, each with different activation energy.

Differential scanning calorimetry (DSC) measurements are reported and initially processed by the Kissinger peak method as, e.g., described by Mittemeijer [4]. The results, if shown in Kissinger's coordinates ($\log(\beta/T^2)$ vs. $1/T$, with the heating rate β, and T as a reference temperature), show reproducible deviations from the expected linear behavior, which cannot be further resolved using this method. An attempt to model the experimental DSC results by a set of independent processes is shown to fail [24]. Additional experiments clearly demonstrate the reproducibility of the experimental results. Four separate isoconversion algorithms are then used to evaluate the data. The resulting activation energy as a function of reaction progress, $E(\alpha)$, is largely identical for all algorithms, while the issue of nonlinearities remains. It is specifically these nonlinearities that indicate significant changes of the effective reaction mechanism as the heating rate changes. Thus, similarity in the shapes of $E(\alpha)$ dependencies obtained from different isoconversion methods does not ensure that the found $E(\alpha)$ represents the actual reaction sequence accurately. It is concluded that for complex reactions, such as the thermite reactions considered in this paper, the number of heating rates required for a meaningful isoconversion processing must be much greater than 3 or 4 considered in many recent studies [20,25–27]. For the specific reactions addressed in this paper, it is shown that isoconversion processing does not lead to a straightforward result even when a greater number of heating rates are used so that development of a reaction model is imperative for practical interpretation of the respective DSC results.

2. Materials

Nanocomposite powders were prepared using a shaker mill (8000D series by Spex Certiprep) with flat-ended steel vials and 3/16″ diameter steel milling balls. Powders of elemental aluminum (99% pure, −325 mesh by Alfa Aesar) and molybdenum trioxide MoO$_3$ (99.95% pure, by Alfa Aesar) were blended in the required proportion. Batches of 5 g were milled under argon and with 4 ml of hexane (C$_6$H$_{14}$) as process control agent to inhibit cold welding and prevent reaction of Al with MoO$_3$ during milling. A constant milling time of 30 min was used. The product powders had particle sizes in the range of 1–200 μm. Each particle consisted of an aluminum matrix with embedded nano-inclusions of MoO$_3$. A cross-section of a particle is shown in Fig. 1.
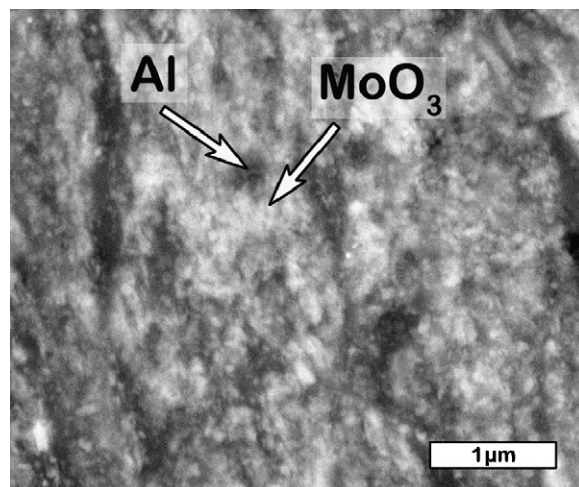

Fig. 1. Backscattered electron image of the cross-section of an Al–MoO$_3$ nanocomposite. Brighter areas correspond to MoO$_3$, and darker areas are Al.

2.1. Thermal analysis

Reactions in the nanocomposite powders at elevated temperatures were studied by DSC using a Netzsch Simultaneous Thermal Analyzer STA409 PC. Alumina pans were used and the furnace was flushed with argon at approximately 50 ml/min. DSC traces were recorded between room temperature and 1200 K with heating rates varying from 1 to 40 K/min. At 1200 K, the samples were held for 30 min, and then cooled to room temperature. In order to establish a useful baseline, the reacted samples were heated again to 1200 K without opening the DSC, or disturbing the sample. The temperature and the sensitivity of the DSC were calibrated with the melting points of a set of high-purity standards at a heating rate of 10 K/min. The temperature measurements are estimated to be accurate within ±1 K. It was furthermore determined that the temperature calibration factors change slightly (and monotonously) with heating rate within the same ±1 K range.

The results of the DSC measurements for a set of heating rates are shown in Fig. 2. The traces show a series of overlapping exothermic peaks. Initial exothermic events starting at ∼400 K are difficult to separate. These features are followed by stronger and more easily identifiable peaks in the 800–950 K temperature range. In addition to the expected shift to higher temperatures at higher heating rates, the shapes of the observed peaks change substantially. For example, a relatively strong peak observed between 600 and 700 K at the lowest heating rates can hardly be detected when heating rates exceed 5 K/min.

2.2. Data processing

In an initial attempt to separate DSC peaks, and to assign individual activation energies, apparent peak maxima were used to process the data according to Kissinger's method [4]. The Kissinger formalism states that

$$\ln\left(\frac{\beta}{T_p^2}\right) = -\frac{E}{RT_p} + C \tag{1}$$

where β is the heating rate, T_p the temperature at the highest reaction rate – taken as the temperature of the peak maximum, E is the activation energy of the process, and R is the universal gas constant. A plot of the left hand side (LHS) of Eq. (1) vs. the reciprocal peak temperature should yield a straight line with the slope of E/R. The constant C is regarded as specific to the reaction mechanism, and
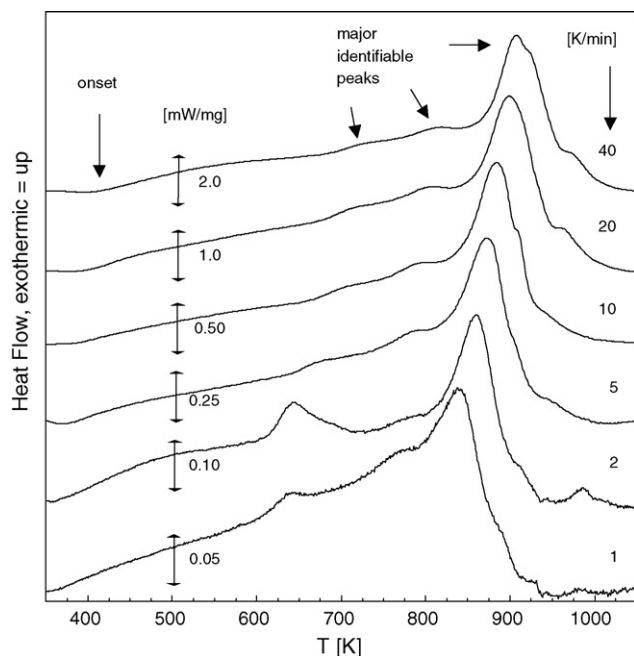
Fig. 2. Baseline-corrected DSC traces collected for nanocomposite powder with bulk composition 4Al + MoO₃ at heating rates ranging from 1 to 40 K/min. The traces are scaled to fit on the same plot; the vertical scale applicable to each trace is shown in units of mW/mg.

Fig. 3. Data processed according to the Kissinger peak position method. Heating rates used were 1, 2, 5, 10, 20, and 40 K/min.

need not be further specified in order to determine E. To apply this method, reaction rate maxima, i.e. peak positions, need to be identified. However, despite the original derivation of Eq. (1) based on the reaction rate, the same equation can be derived using points of constant reaction progress under different linear heating conditions, see, e.g. ref. [4]. One can then assume that other reference points also reflect states of constant reaction progress. This reasoning has been used in the derivation of kinetic parameters with peak onsets [29,30] or inflection points [31] as reference temperatures. As can be seen in Fig. 2, in the present case only the peak in the 800–900 K range can be tracked throughout all measurements. In order to be able to estimate the activation energy for the other identifiable features in the measurements, different reference points were used as approximations. Specifically, the onset point of the overall heat effect was used, as well as the inflection point of the minor peak in the 600–700 K range. The onset was determined as the intersection between the initial baseline and the low-T slope of the signal; the inflection points were taken as the peak maxima of the first derivative of the DSC signal. Fig. 3 shows the results. It is evident that within these few measurements, some apparent outliers exist, and that straight line fits to the data are therefore questionable. Results that are qualitatively similar have been reported in other publications on energetic composites [20,26–28]. Additional experiments were performed in smaller heating rate increments in order to confirm or rule out reproducibility issues. The results suggest that such "outliers" consistently form a trend. The values of E determined therefore have to be regarded with caution, and more detailed processing is needed.

Since simple peak processing leads to the conclusion that individual peaks cannot be assigned unique activation energy values, it was next attempted to determine the activation energy as a function of reaction progress according to various isoconversion formalisms. In all these methods, the reaction progress, α, is determined at a number of different heating rates by integration of the heat flow Φ over time. This requires a reliable determination of the baseline of the measurements. Despite the experimental pro-
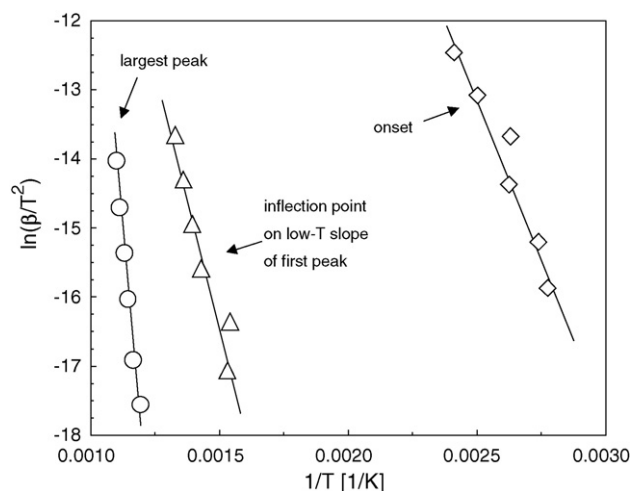
cedure outlined above, the signal at the end of the measurement ($T > 1000$ K) did not always return to zero, indicating that the baseline correction based on the repeated heating of the reacted sample was not complete. This is most likely due to slight changes in the physical parameters of the sample that affect heat transfer, such as shrinkage or changes in porosity. The high-temperature limit for the determination of the total reaction heat and the reaction progress was chosen as the point after which the signal was essentially constant. The low-temperature limit was more easily recognized as a clear onset point, see Fig. 2 for comparison. However, as mentioned above, features in the low-temperature region of the measurement are difficult to resolve, and questions may arise as to whether the gradually increasing signal may be an artifact. In an earlier investigation on the same type of nanocomposite thermite, partially reacted material was recovered after heating to 593 K and analyzed by X-ray diffraction [23]. The results showed that the amount of MoO₂ increased from 1.5 to 3.1 mol% between the as-prepared and the partially reacted nanocomposite. Similarly, the amount of free Al decreased from 67.3 to 65.2 mol%. Any amorphous reaction products, especially aluminum oxide, could not be quantified by XRD – nonetheless, the result confirms that there is a measurable reaction progress even below 600 K.

A synthetic baseline Φ_{BL} was then constructed by taking the weighted average between the heat flow at the beginning (Φ_i) and the end (Φ_f) of the experiment with α as the weighing factor [34]:

$$\Phi_{BL} = (1 - \alpha)\Phi_i + \alpha\Phi_f \tag{2}$$

This baseline was subtracted from the measured heat flow, and finally α was calculated as a function of the time, t, by integration from the time t_0 at the beginning of the experiment using u as the integration variable:

$$\alpha(t) = \frac{1}{Q}\int_{t_0}^{t} \Phi(u) - \Phi_{BL}(u)\mathrm{d}u \tag{3}$$

Since the baseline depends on α while α depends on the baseline, α was calculated iteratively. The initial baseline was taken as a straight line between starting and end points; subsequently the value of α converged after less than 10 iterations.

The resulting plot of α vs. temperature is shown in Fig. 4 A for the heating rates 1, 2, 3, and 5 K/min. As the figure shows, adjacent curves intersect with each other, meaning that not all plots of T vs. β at a given degree of conversion, α, are monotonous. This sig-
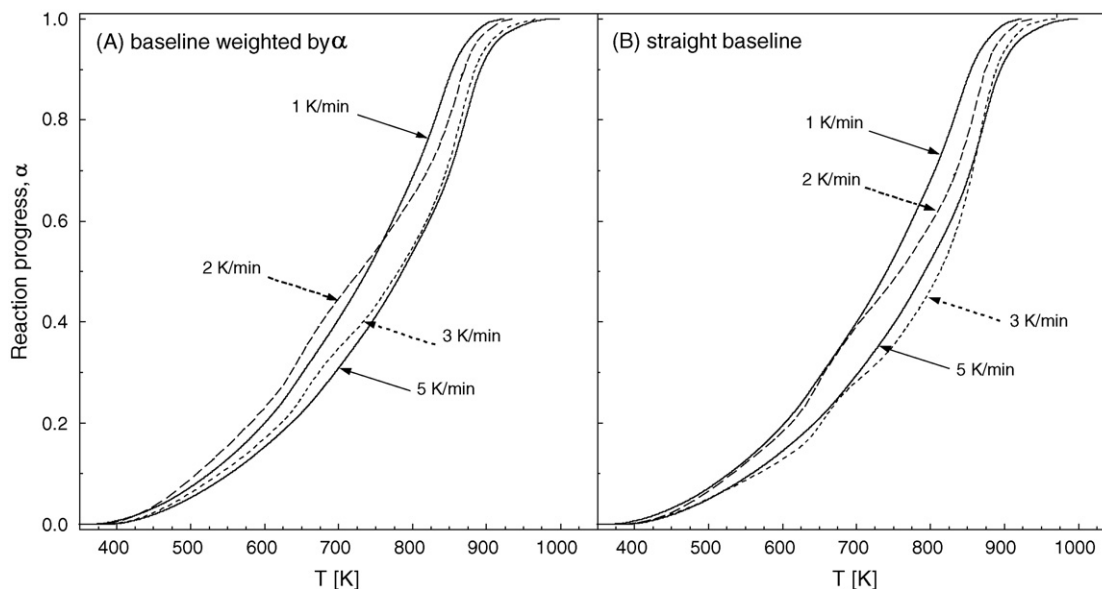
Fig. 4. Plot of reaction progress α vs. temperature after subtraction of a proportional baseline (A), and a linear baseline (B).

nals abnormal kinetic relations. To verify whether this behavior is inherent in the data or an artifact of the baseline construction, an analogous plot is shown in Fig. 4 B, where the onset and endpoints of the measured DSC signals were connected by a straight line, as the simplest case of possible baselines. This demonstrates that while the shape of the $\alpha(T)$ curves are somewhat different compared with Fig. 4 A, curves still intersect, confirming problematic kinetic relations. To verify the reproducibility of experiments, the run at 2 K/min was repeated resulting in an effectively identical DSC trace and respectively the same reaction progress trend as shown in Fig. 4. Naturally, one could construct arbitrary baselines, tailored to give non-intersecting $\alpha(T)$ curves. Some kinetic software solutions actually optimize the baselines of individual measurements in order to ensure monotonous $T_\alpha(\beta)$ curves [10,35]. However, while there may be cases where this is justified, it would impose constraints on the kinetic analysis that would obscure any unusual behavior. In the present case, the proportional baseline as defined in Eq. (2) was used to ensure consistent treatment of all measurements.

To verify that the choice of baseline is reasonable, the total evolved heat is compared for all individual experiments in Fig. 5. Also shown are the calculated values for the reaction enthalpy of complete reduction of MoO$_3$ to Mo, and partial reduction to MoO$_2$. The reaction heat values obtained from different runs are not significantly affected by the heating rate, and fall between the limits of
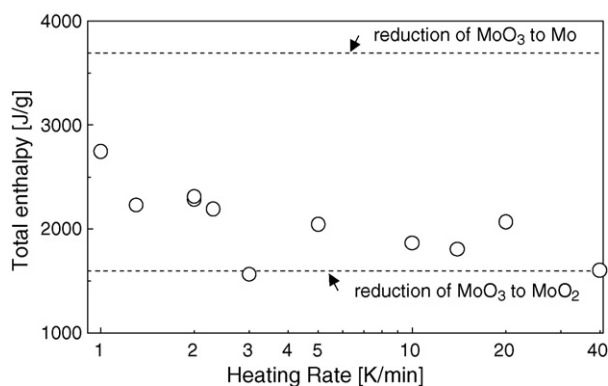

Fig. 5. Total evolved heat for all heating rates.

full and partial reduction of MoO$_3$, confirming that the calculated baselines are acceptable.

A number of different approaches to isoconversion data processing have been developed. The Ozawa–Flynn–Wall, generalized Kissinger, and Starink's methods are examples of isoconversion methods that rely on the approximation of the so-called temperature integral ([1,3,4] see also [5] for a critical summary). Of these examples, Starink's method is the most accurate [5,32,33]. It uses the following equation:

$$\ln\left(\frac{\beta}{T_\alpha^{1.92}}\right) = -1.008\frac{E}{RT_\alpha} + C \tag{4}$$

where T_α is the temperature corresponding to a specific degree of conversion. By plotting the LHS of Eq. (4) vs. 1/T for fixed values of α, the activation energy can be determined as a function of α.

Other methods do not use an approximation of the temperature integral, but instead use the measured heat flow directly. An example is the Friedman method ([2], see also [5]):

$$\ln\left(\frac{d\alpha}{dt}\right) = -\frac{E}{RT_\alpha} + C \tag{5}$$

where explicit knowledge of the heating rate β is not required.

Fig. 6 shows plots of the LHS of Eqs. (4) and (5) vs. 1/T. In both plots, the contours of constant reaction progress cannot reasonably be described by straight lines. In particular, the deviations at low heating rates are strong and reproducible. As noted above, the measurement at 2 K/min (3rd lowest heating rate in Fig. 6) was repeated, and the repeatability is of the same scale as the size of the symbols used in Fig. 6. The consistent trends observed over a range of heating rates strongly suggest that at least over the range of heating rates investigated, a unique activation energy cannot be assigned to a specific degree of reaction progress. Instead, overlapping reactions that likely depend on each other must be considered in order to successfully model the observed DSC measurements.

Both methods described so far yield plots of contour lines of constant α values as intermediate results, which ideally should be straight lines, where the slope is determined by E/R. This allows a visual assessment of inconsistencies, such as the already mentioned nonlinearities observed at low heating rates. Vyazovkin [6] has developed an approach that is based on finding an approximate
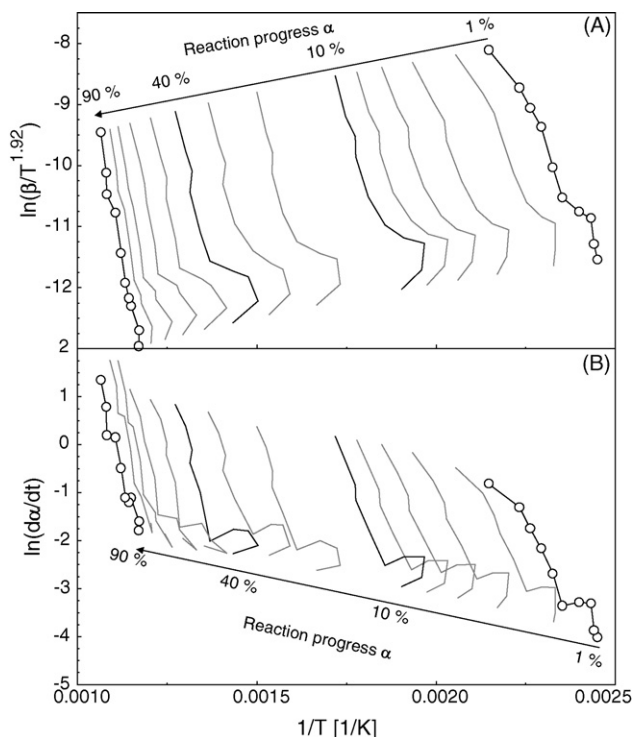
Fig. 6. Isoconversion processing of DSC measurements to determine the activation energy as a function of the reaction completeness. Top (A): Starink, Bottom (B): Friedman.

solution to the following set of equations instead of straight-line fits:

$$\frac{A}{\beta_i} \int_0^T \exp\left(\frac{-E_i(\alpha)}{RT}\right) dT = \frac{A}{\beta_j} \int_0^T \exp\left(\frac{-E_j(\alpha)}{RT}\right) dT \tag{6}$$

where the indices i and j refer to experiments with different linear heating rates. Instead of integrating over the temperature, one can integrate over time, while treating the temperature as an (experimentally measured) function of the time. This obviates the need for strict linear heating programs, and removes inaccuracies introduced by deviations from linearity such as might occur due to self-heating or self-cooling of the sample during exothermic, or endothermic events, respectively.

In a further development, Vyazovkin [7] suggested to modify Eq. (3), by integrating the DSC signal piecewise, and segmenting the measured curve in as many parts as points at which $E(\alpha)$ is to be determined.

$$\alpha(t) = \frac{1}{Q} \int_{t_1}^t \Phi(u) - \Phi_{BL}(u) du \tag{7}$$

where Q is the integrated heat effect between the boundaries t_1 and t_2:

$$Q = \int_{t_1}^{t_2} \Phi(u) - \Phi_{BL}(u) du \tag{8}$$

and $t_1 < t < t_2$. This has the advantage that features of the DSC signal at progressively larger values of α are not affected by earlier features – as they are when Eq. (3) is used.

Fig. 7 shows the activation energy as a function of α, determined by all the above-described methods. It is apparent that mechani-
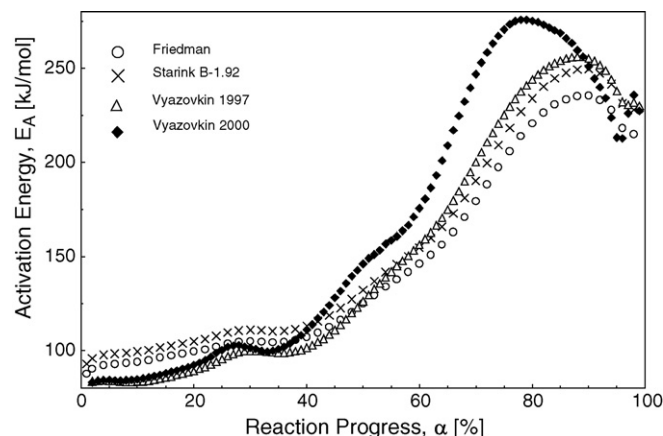

Fig. 7. Activation energy as a function of reaction progress as determined by Friedman's, Starink's and Vyazovkin's isoconversion methods.

cal application of these isoconversion methods gives very similar results that appear to be consistent with one another, regardless of the nonlinearities evident in Fig. 6A and B. The fact that Vyazovkin's methods [6,7] give substantially the same results attests that the methods are functionally equivalent. However, the consistency between results of different isoconversion techniques does not indicate that the activation energy as a function of α has been accurately determined.

It may be possible to devise a strategy to separate the measurements into groups or ranges of heating rates where the assumption of linearity (in the case of the "traditional" isoconversion approaches) is valid. The approaches based on linear fits allow a correlation coefficient to be calculated for each line fit, that shows the level of confidence of the value of $E(\alpha)$ at a given degree of conversion α. As the correlation coefficient decreases below unity, the confidence level also decreases.

In both variations of Vyazovkin's method, the system of Eq. (6) is solved approximately by minimizing the following expression [7]

$$\sum_i \sum_{j \neq i} \left(\frac{\beta_j \int_0^T \exp\left(\frac{-E_i(\alpha)}{RT}\right) dT}{\beta_j \int_0^T \exp\left(\frac{-E_j(\alpha)}{RT}\right) dT} \right) \tag{9}$$

This minimum can be normalized to the value that it would assume for an exact solution of the system of Eq. (6). The inverse of this normalized minimum projects, like the correlation coefficients, to values between 0 and 1. This can now qualitatively be compared to the correlation coefficients of the traditional isoconversion methods. As with the correlation coefficients, a value significantly below unity indicates lower confidence levels. This basic idea is sufficient to identify subsets of heating rates for which linearity can safely be assumed, however it has been developed further to calculate proper confidence intervals for the activation energies so determined [36].

These error metrics (correlation coefficient for Starink's and Friedman's methods, and inverse, normalized value of minimum (9) for Vyazovkin's methods) are shown in Fig. 8. It is now possible to systematically eliminate measurements at low, or high heating rates, respectively, to identify regions where the assumption of linearity (Starink and Friedman) hold, and where the minimum (9) is consistently close to its ideal value.
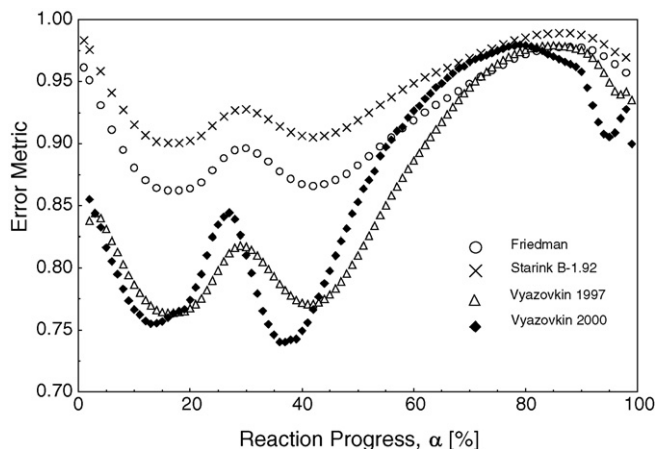
Fig. 8. Error metrics calculated for all considered isoconversion methods.

For the complete set of measurements, the only region where the activation energy is consistently determined with high confidence, is the range $\alpha = 70$–90%. Values below $\alpha = 50$% are relatively the most unreliable. It is likely that the strongest peak in the DSC measurements between 800 and 900 °C dominates in that region, even though smaller peaks are clearly visible on its high-temperature side. Similarly, up to about 5% conversion the error metrics are relatively high while the activation energy is nearly constant at about 95 kJ/mol. This may be indicative of a single process with an identifiable activation energy limiting the rate of the reaction in its very initial stages. Conversely, the relatively uniform feature following around 10–25% of conversion is a composite of various unresolved contributions, which is poorly reflected in the $E(\alpha)$ results.

3. Conclusions

Analysis of exothermic reactions in Al–MoO$_3$ system shows that kinetics of such reactions cannot be meaningfully determined by isoconversion processing. A data set comprising five heating rates was initially processed neglecting what appeared to be a minor nonlinearity in isoconversion plots. Application of a simplified isoconversion method yielded several activation energies, consistent between different methods. However, the results turn out to be incorrect once experiments at additional heating rates showed that the minor nonlinearity neglected in the initial processing is not an experimental error, but instead represents an actual trend. Documenting this trend effectively voided any isoconversion processing based on the obtained set of DSC measurements.

For the Al–MoO$_3$ thermite system, the shapes of functions of activation energy depending on reaction progress, $E(\alpha)$, are similar to one another when different isoconversion techniques are applied, including some of the most recent and advanced algorithms. It is concluded that the similarity in the shapes of $E(\alpha)$ obtained from different isoconversion techniques does not support or justify these shapes as accurate.

The data processing for the specific materials system addressed in this paper shows that activation energy cannot be meaningfully determined as a function of reaction progress, as would be

required for any type of model-free processing. In this case, which is expected to represent a rather common situation for solid state reactions with many intermediate products, many measurements at different heating rates are needed to identify trends, and a detailed model development is necessary for meaningful description of the reaction kinetics. Generally, there is no rigorous a-priori indication as to whether isoconversion processing is applicable to a specific complex reaction. It appears that the only way to determine this, is to perform the experiments and to evaluate the error metrics.

Acknowledgements

References

[1] H.E. Kissinger, Anal. Chem. 29 (1957) 1702.
[2] H.L. Friedman, J. Polym. Sci. C 6 (1964) 183.
[3] T. Akahira, T. Sunose, Res. Report Chiba Inst. Technol. 16 (1971) 22–31.
[4] E.J. Mittemeijer, J. Mater. Sci. 27 (1992) 3977.
[5] M.J. Starink, Thermochim. Acta 404 (2003) 163–176.
[6] S. Vyazovkin, J. Therm. Anal. 49 (1997) 1493.
[7] S. Vyazovkin, J. Comput. Chem. 22 (2) (2001) 178–183.
[8] R. Serra, J. Sempere, R. Nomen, Thermochim. Acta 316 (1) (1998) 37–45.
[9] P. Budrugeac, E. Segal, J. Therm. Anal. Calorim. 72 (2003) 831–837.
[10] Advanced Kinetics and Technology Solutions: http://www.akts.com (AKTS-Thermokinetics software and AKTS-Thermal Safety software).
[11] Perkin Elmer: http://www.perkinelmer.com (Pyris Advanced Kinetics Software).
[12] J. Opfermann, NETZSCH Thermokinetics 2, Version 2005.04 NETZSCH Gerätebau GmbH.
[13] A.K. Burnham, R.L. Braun, Energy Fuels 13 (1999) 1–22.
[14] A.K. Burnham, L.N. Dinh, J. Therm. Anal. Calorim. 89 (2007) 479–490.
[15] A.K. Galwey, Thermochim. Acta 397 (2003) 249–268.
[16] S. Vyazovkin, Thermochim. Acta 397 (2003) 269–271.
[17] M.E. Brown, J. Therm. Anal. Calorim. 82 (3) (2005) 665–669.
[18] T.M. Tillotson, A.E. Gash, R.L. Simpson, L.W. Hrubesh, J.H. Satcher Jr., J.F. Poco, J. Non-Crystalline Solids 285 (1–3) (2001) 338–345.
[19] D.S. Moore, S.F. Son, B.W. Asay, Propellants, Explosives, Pyrotechnics 29 (2) (2004) 106–111.
[20] K.J. Blobaum, M.E. Reiss, J.M. Plitzko Lawrence, T.P. Weihs, J. Appl. Phys. 94 (5) (2003) 2923–2929.
[21] J.J. Granier, M.L. Pantoya, Combust. Flame 138 (2004) 373–383.
[22] M. Schoenitz, T.S. Ward, E.L. Dreizin, Proc. Combust. Inst. 30 (II) (2005) 2071–2078.
[23] S.M. Umbrajkar, M. Schoenitz, E.L. Dreizin, Propellants, Explosives, Pyrotechnics 13 (5) (2006) 382–389.
[24] S.M. Umbrajkar, PhD thesis, NJIT, 2007.
[25] S.M. Umbrajkar, M. Schoenitz, E.L. Dreizin, Thermochim. Acta 451 (2006) 34–43.
[26] E.M. Hunt, M.L. Pantoya, J. Appl. Phys. 98 (3) (2005) 1–8.
[27] J. Sun, M.L. Pantoya, S.L. Simon, Thermochim. Acta 444 (2) (2006) 117–127.
[28] S.M. Umbrajkar, M. Schoenitz, E.L. Dreizin, J. Propulsion Power 23 (4) (2007) 683–687.
[29] V.A. Khonik, K. Kitagawa, H. Morii, J. Appl. Phys. 87 (12) (2000) 8440–8443.
[30] Y.X. Zhuang, W.H. Wang, Y. Zhang, M.X. Pan, D.Q. Zhao, Appl. Phys. Lett. 75 (16) (1999) 2392–2394.
[31] K. Cheng, Mater. Sci. Eng. B: Solid-State Mater. Adv. Technol. B60 (3) (1999) 194–199.
[32] M.J. Starink, J. Alloys Compd. 433 (2007) L4–L6.
[33] M.J. Starink, Int. Mater. Rev. 49 (2004) 191–226.
[34] W.F. Hemminger, S.M. Sarge, J. Therm. Anal. 37 (1991) 1455–1477.
[35] B. Roduit, C. Borgeat, B. Berger, P. Folly, B. Alonso, J.N. Aebischer, F. Stoessel, J. Therm. Anal. Calorim. 80 (2005) 229–236.
[36] S. Vyazovkin, C.A. Wight, Anal. Chem. 72 (2000) 3171–3175.